

Tubulin Binding, Protein-Bound Conformation in Solution, and Antimitotic Cellular Profiling of Noscapine and Its Derivatives

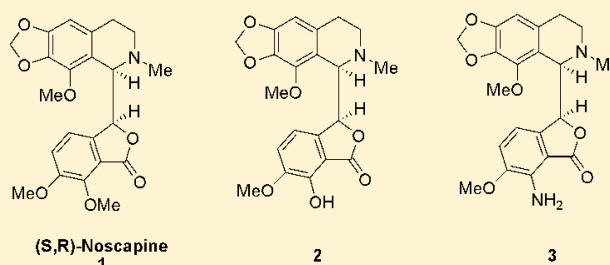
Youssef L. Bennani,^{†,*} Wenxin Gu,[†] Angeles Canales,[‡] Fernando J. Díaz,[§] Brenda K. Eustace,[†] Russell R. Hoover,[†] Jesus Jiménez-Barbero,[§] Azin Nezami,[†] and Tiansheng Wang[†]

[†]Vertex Pharmaceuticals Inc., 130 Waverly Street, Cambridge Massachusetts 02139, United States

[‡]Departamento Química Orgánica I, Facultad Ciencias Químicas, Universidad Complutense de Madrid, Avenida Complutense s/n, 28040 Madrid, Spain

[§]Department of Physical Chemistry, Centro de Investigaciones Biológicas, Consejo Superior de Investigaciones Científicas, Ramiro de Maeztu 9, 28040 Madrid

ABSTRACT: Noscapine and its 7-hydroxy and 7-amino derivatives were characterized for their binding to tubulin. A solution NMR structure of these compounds bound to tubulin shows that noscapine and its 7-aniline derivative do not compete for the same binding site nor does its small molecule crystal structure match its tubulin-bound conformation. These compounds were also tested for their antiproliferative effects on a panel hepatocellular carcinoma cell lines.



1. INTRODUCTION

Noscapine **1** is a naturally occurring phthalideisoquinoline alkaloid obtained in about 7% during opium harvesting.¹ It has been used in humans as an oral antitussive agent and displays a favorable toxicity profile.² Additionally, it has been known for some time that **1** can act as a weak anticancer agent in certain in vivo models.³ Recently, Joshi et al. have performed several studies to evaluate the mechanism of action of this anticancer effect and found that compound **1** can disrupt tubulin dynamics.⁴ Over the past few years, several studies covering **1** and some of its derivatives in oncology have been reported.⁵ Despite its weak antimitotic activity, compound **1** has entered human testing, and is now in phase 2 clinical studies for cancer treatment.⁶ In earlier communications, we have reported on two types of derivatives thereof. First, enantiomerically pure 7-O-alkyl and aryl derivatives that stop cells in G1/S stage,⁷ and second, 7-phenol **2** and aniline **3** derivatives that mirror compound **1** cellular phenotype and causing the arrest of rapidly dividing cells in G2/M stage at about 500 times increased potency when compared to **1** (Figure 1).⁸

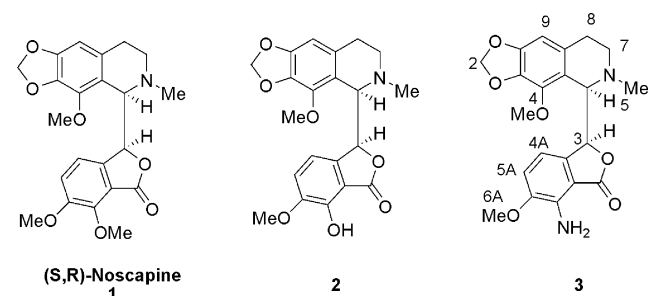


Figure 1. Noscapine and its derivatives.

Herein, we wish to report on the biochemical characterization of these compounds with tubulin and their antimitotic effects in hepatocellular carcinoma cell lines. The following three sections cover (1) tubulin binding site investigations of **1** and its derivatives **2** and **3**, (2) solution NMR of tubulin bound to **1**, as well as compound **3**, and (3) antiproliferative effects of these compounds on 16 hepatocellular carcinoma cell lines.

2. TUBULIN BINDING ASSAYS

To test if the previously observed cytotoxic effect of these compounds is due to interactions with tubulin, we used a microtubule assembly assay with purified tubulin. The assembly inhibition properties of the compounds were tested in glycerol assembly buffer (GAB), 3.4 M glycerol, 10 mM sodium phosphate, 1 mM EGTA, 0.1 mM GTP, 6 mM and MgCl₂, pH 6.7. Under these conditions, tubulin assembles into microtubules with a critical concentration⁹ of 3.3 μM. In this assay, a 15 μM concentration of tubulin was employed with the expectation that in the absence of any compound, tubulin polymerizes (at about 11.7 μM) to form pellets. As it can be seen in Figure 2, compound **3** is a very potent substoichiometric assembly inhibitor, reducing the amount of pelleted tubulin to 50% at a concentration around 1 mM (EC₅₀ = 1.2 ± 0.3 μM), while noscapine does not inhibit tubulin assembly under this assay conditions. Compound **2** is a weak inhibitor requiring stoichiometric amounts to reduce the amount of polymer formed. It is worth noting that we detected stability problems for this derivative that preclude further studies on this compound.

Received: June 30, 2011

Published: February 9, 2012

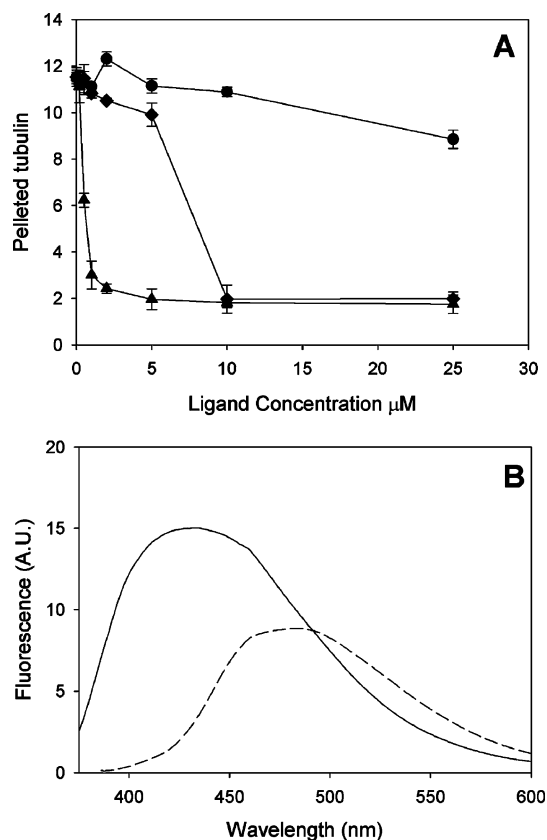


Figure 2. (A) Inhibition of tubulin assembly by noscapine analogues (circles 1, diamonds 2, triangles 3). All data is average of three experiments, error bars are standard errors. (B) Fluorescence emission spectra of 10 μM 3 in 10 mM sodium phosphate 0.1 mM GTP buffer, pH 7.0, 25 $^{\circ}\text{C}$, in the presence (solid line) and absence (dashed line) of 10 μM tubulin.

From the stoichiometry and the measured binding constant below (for compound 3), 0.87 μM protein was bound to the ligand, accounting for a 3.5% of the total protein content. These data suggest that the compound is a strong sub-stoichiometric inhibitor of tubulin assembly.

To further characterize and establish a binding constant for these compounds to tubulin, we used fluorescence spectroscopy in the presence and absence of tubulin. Compound 3 shows an absorption band in the near UV centered at 341 nm ($\epsilon_{341} = 6600 \text{ M}^{-1} \text{ cm}^{-1}$). This compound is fluorescent with an emission maximum at 465 nm. Upon incubation with tubulin, the emission maxima of the compound shifts to blue (425 nm), increasing ~ 11 times its fluorescence at 425 nm. The anisotropy of the compound fluorescence in the absence of tubulin is 0.02, typical for an unbound ligand. This parameter largely increases (0.18) upon tubulin addition, indicating binding to tubulin (Figure 2B). Compounds 1 and 2 have similar spectroscopic properties (2 $\epsilon_{\text{max}337} = 13900 \text{ M}^{-1} \text{ cm}^{-1}$ emission maximum at 475 nm, 1 $\epsilon_{\text{max}317} = 2800 \text{ M}^{-1} \text{ cm}^{-1}$ emission maximum at 420 nm) as free or unbound ligands. However, they do not change fluorescence intensity or anisotropy upon incubation with tubulin (10 μM), indicating that any possible binding to the protein is weak. The change in the fluorescent properties of compound 3 can be then employed to monitor the binding state of the compound and the number of binding sites on tubulin dimers. First, 5 μM tubulin was titrated with growing amounts of derivative 3 up to 100 μM and the amount of bound and

free compound was quantified by employing the change in fluorescence properties of the compound upon binding to tubulin (Figure 3). The number of binding sites of the

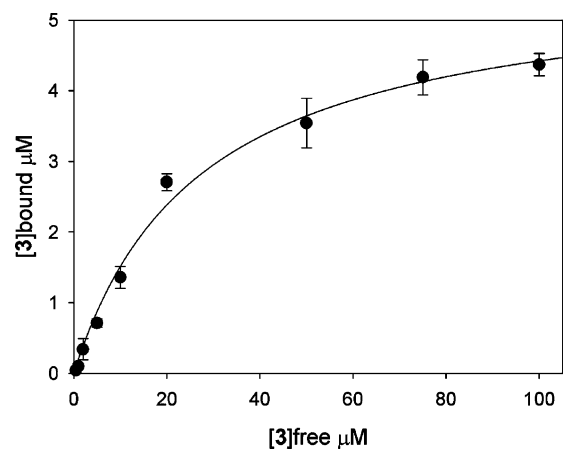


Figure 3. Titration of 5 μM tubulin in 10 mM sodium phosphate 0.1 mM GTP buffer, pH 7.0, 25 $^{\circ}\text{C}$, with growing amounts of 3. All data are average of three experiments, error bars are standard errors.

compound 3 in the tubulin dimer was found to be 0.87 ± 0.03 sites, indicating a single site and a 1:1 stoichiometry.

Second, 5 μM of compound 3 was titrated with growing amounts of tubulin up to 100 μM , and the amount of bound and free compound was quantified by employing the change of fluorescence properties of the compound upon binding to tubulin (Figure 4). The binding constant was calculated,

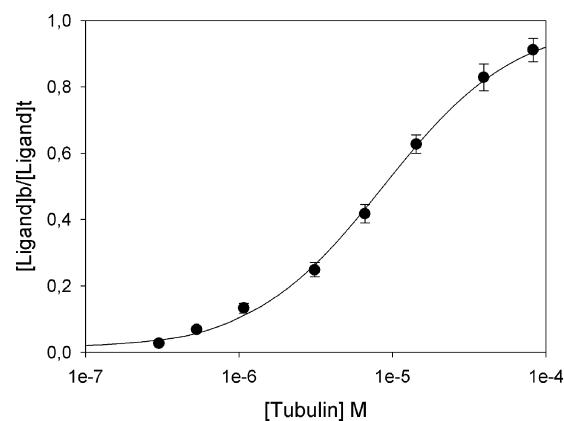


Figure 4. Titration of 5 μM of compound 3 in 10 mM sodium phosphate 0.1 mM GTP buffer, pH 7.0, at 25 $^{\circ}\text{C}$, with growing amounts of tubulin. All data are average of five experiments, error bars are standard errors.

assuming a single site a 1:1 stoichiometry and 0.87 ± 0.03 sites per tubulin dimer, to be $1.15 \pm 0.06 \times 10^5 \text{ M}^{-1}$ at 25 $^{\circ}\text{C}$.

Finally, we tested the influence of Mg^{2+} on compound 3 binding to tubulin (Figure 5). As such, 5 μM of compound 3 was titrated with growing amounts of tubulin up to 100 μM in the presence of 0, 0.5, and 2 mM MgCl_2 ; the amount of bound and free compound was quantified by employing the change of fluorescence properties of the compound upon binding to tubulin (Figure 5). The binding constant was identical for all concentrations assayed, indicating that the binding site is not

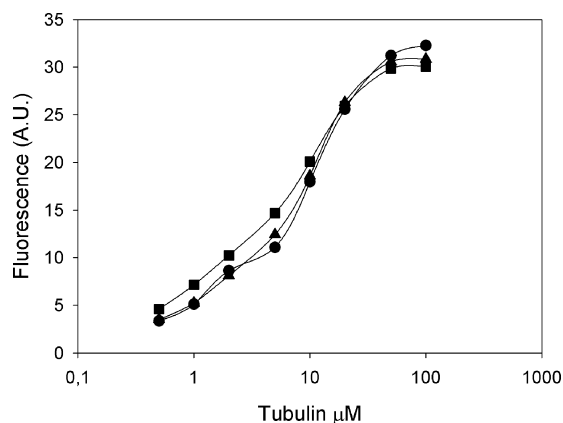


Figure 5. Titration of 5 μM of compound 3 in 10 mM phosphate 0.1 mM GTP buffer, pH 7.0, at 25 $^{\circ}\text{C}$, with growing amounts of tubulin in the presence of 0 (solid circles), 0.5 (solid squares), and 2 mM MgCl_2 (solid triangles). All data are average of three experiments.

affected by oligomerization state as it would be expected if it is located in the intradimer space as for colchicine.¹⁰

The same change in the fluorescent properties of compound 3 can be used to check for competition with tubulin assembly inhibitors of the vinca and colchicine binding sites. Competition assays in which 10 μM tubulin and 10 μM of compound 3 were incubated with up to 100 μM of Podophyllotoxin, Vinblastine, and Isohomohalichondrin or up to 20 μM of Pironetin or Gossipol. No change in the fluorescent properties of aniline 3 was observed, indicating that these compounds are not competing for the same site. Additionally, excess (50 μM) of the weakly fluorescent compound (1) does not modify the observed fluorescence of the solution, indicating a much lower affinity for the site. On the other hand, under similar conditions (vide supra), incubation with up to 50 μM of nocodazole results in slow decrease of the fluorescence observed (Figure 6),

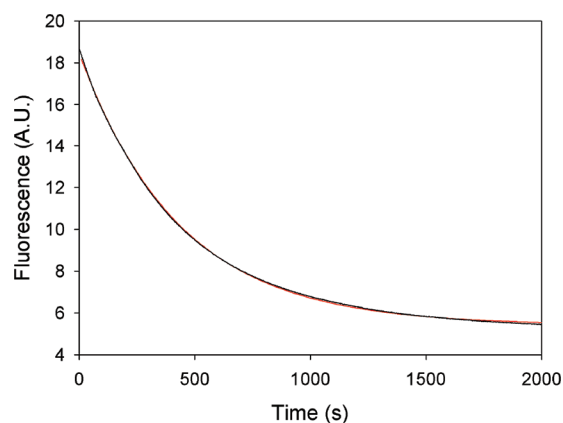


Figure 6. Nocodazole induced dissociation of 10 μM of compound 3 from 10 μM tubulin in 10 mM sodium phosphate 0.1 mM GTP buffer, pH 7.0, at 25 $^{\circ}\text{C}$. At time 0, 50 μM nocodazole was added to the solution. Black line experimental data. Red line fitting.

indicated a possible effect on binding at least partially to the same site. Because Nocodazole binding to tubulin is fast, the result implies that dissociation of compound 3 is slow. The observed kinetics of dissociation shows a single phase (which indicates a single type of binding site) with an apparent rate constant of $2.3 \times 10^{-3} \text{ s}^{-1}$ at 25 $^{\circ}\text{C}$. Nocodazole is a synthetic aminobenzimidazole with antimitotic and antitumoral activity

whose target is tubulin.¹¹ It binds to tubulin with an affinity of $4 \times 10^5 \text{ M}^{-1}$ in the same order of magnitude as compound 3. Binding of Nocodazole to tubulin affects colchicine binding, which indicates that its binding site should be close of that of colchicines, between the α and β tubulin subunits. While the exact binding site of compound 3 has not been precisely mapped, it is possible that (a) it overlaps both colchicines and nocodazole binding sites or (b) it binds to a new site, access to which is dramatically affected in the presence of nocodazole (tubulin-X-ray based computer generated models were relatively inconclusive in attempts to dock nocodazole, colchicine, and compound 3).

3. STD NMR EXPERIMENTS

Saturation transfer difference (STD) experiments have been acquired with freshly prepared tubulin α/β heterodimer solutions in the presence of 1, using a ligand/protein molar ratio 30:1 (300 mM noscapine, 10 mM dimeric tubulin). STD spectra provided clear enhancements for the proton signals of the molecule, confirming that noscapine is recognized by the tubulin heterodimer. STD spectrum of the derivative 3 was carried out under the same conditions, showing also clear STD effects for the ligand protons. STD competition experiments were performed in order to assess whether both compounds are recognized by the same protein-binding site. Addition of aniline 3 to a sample containing 1 and tubulin α/β heterodimer does not decrease the STD signals of 1. Therefore, these compounds do not compete for the same site. This observation is in agreement with our biochemical data that reveal aniline 3 as an inhibitor of tubulin assembly, whereas 1 is not able to produce the same inhibition effects. Thus, the STD effect observed from 1 could be assigned to a nonspecific low affinity interaction.

In the case of aniline 3, the larger STD effects were detected for the protons located at the aromatic rings (H5A, H4A, H9, and OCH_3 4), being the highest values the STDs of the proton and methyl group in the aromatic ring attached to the 1,3-oxolane ring, H9 and OCH_3 (4) (19%) (For NMR assignment of 1 and 3, please see Figure 1, Figure 7, and Table 1).

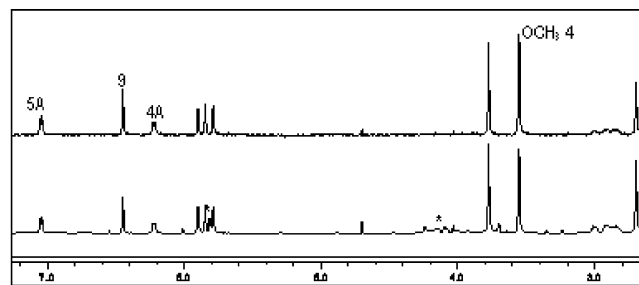


Figure 7. STD, (top spectrum) and off resonance spectrum (bottom, reference spectrum acquired without protein irradiation) of 3 in the presence of dimeric tubulin. *Signals of GTP that is added in the buffer for improvement of protein stability.

Transferred NOE experiments of compound 3 were also performed. Strong negative NOE cross peaks were observed for 3 in the presence of the tubulin α/β heterodimer; these cross peaks indicate binding of the molecule to the tubulin preparation (the 500 MHz NOESY cross-peaks were moderately positive at 298 K for the free ligand). Atoms H3 and H5 NOE contacts are key cross peaks in the study of ligand conformation

Table 1. NMR Signal Assignment in Water^a

	δ (ppm) D ₂ O	
	3	Noscapine (1)
H5A	7.17 (d)	7.42
H4A	6.33 (d)	6.99
H9	6.66 (s)	6.46
H3	6.0	5.96
H2	5.96 and 5.90	5.83 and 5.75
H5	4.96	4.80
OMe (6A)	3.89	3.85
OMe (7A)		3.81
OMe (4)	3.67	3.46
H7	3.09 and 2.99	3.13 and 2.93
NMe	2.79	2.68
H8	2.95 and 2.74	2.85 and 2.69

^a10 mM sodium phosphate, 0.1 mM GTP, D₂O.

because the C3–C5 bond is the main point of flexibility or rotation in these derivatives of 1. The presence of clear NOEs between H3–H7, H3–NCH₃, and H5–H4A proton pairs in the TR-NOESY experiment points out that the bound conformation of 3 is different from that of the conformer crystallized for the phenol derivative 2. Distances in the crystal are 4.8, 4.2, and 4.4 Å, respectively. Therefore, absence or very weak NOEs are expected between H3–H7, H3–NCH₃, and H5–H4A. In contrast, medium intensity NOE peaks are observed for these protons even at low mixing times (100 ms). NMR experiments were further supported by molecular mechanics calculations performed by using the Maestro 7.5 package and OPLS 2005 force field. The conformational searches were carried out with 20000 steps of the usage-directed Monte Carlo/energy minimization (MC/EM) procedure. The starting compound 3 coordinates were built from the X-ray structure of phenol derivative 2. The lowest energy structures found in the conformational search showed a different orientation of the rings around C3–C5 torsion than the one observed in the crystal structure (Figure 8 middle panel). The interproton distances of

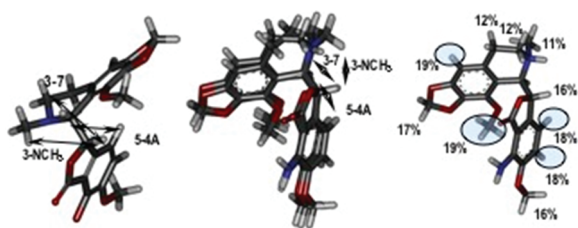


Figure 8. Left panel: phenol 2 X-ray crystal structure. Middle panel: aniline 3 lowest energy structures obtained in the conformational search, three conformers overlaid. Right panel: STD effects mapped on the bound conformation of 3, protons with the highest STD effects are marked with blue circles.

this family of conformers are in agreement with the NOE contacts observed by NMR.

In the case of aniline 3, the larger STD effects were detected for the protons located at the aromatic rings (H5A, H4A, H9, and OCH₃ 4), being the highest values the STDs of the proton and methyl group in the aromatic ring attached to the 1,3-oxolane ring, H9, and OCH₃ 4 (19%).

NMR spectroscopy allowed the detection of compound 3 and 1 binding to tubulin α/β heterodimer. However, according

to STD competition experiments, these compounds do not compete for the same binding site. These results are in agreement with the different activities detected for both derivatives 2 and 3 in the inhibition of tubulin polymerization. The bound conformation of compound 3 was determined by using TR-NOESY experiments assisted by molecular mechanics calculations. The epitope mapping of the aniline derivative was also carried out by using STD techniques showing the ligand regions more involved in tubulin recognition. The larger STD effects map the ligand epitope, which comprises the protons located at the aromatic rings (H5A, H4A, H9, and OCH₃ 4), showing the highest values of STDs the proton and methyl group in the aromatic ring attached to the 1,3-oxolane ring, H9, and OCH₃ 4 (19%).

4. CELLULAR ANTIPROLIFERATION STUDIES

Compounds 1–3 were tested first in cellular viability assays using two hepatocellular carcinoma cell lines (SNU398 and PLC/PRF/5). Compound 3 caused a potent decrease in cell viability with IC₅₀s of 94.3 and 237.4 nM in SNU398 and PLC/PRF/5, respectively. Compound 1 and phenol 2 both displayed IC₅₀s greater than 2 μ M in this assay. Then similar results were seen when 1 and 3, along with three chemotherapeutics Docetaxel, Epothilone B, and Vincristine (which all affect microtubule dynamics), were tested against 16 HCC cell lines (Table 2). To determine whether the observed inhibition of cell

Table 2. HCC Cell Lines Assays of 1 and 3^a

	IC ₅₀ (nM)				
	Noscapine (1)	3	Docetaxel	Epothilone B	Vincristine
SMMC-7721	>1000	109.3	2	2.3	6.5
MHCC97H	>1000	351	22.4	6.7	21.2
Bel-7402	>1000	78.4	1.9	0.9	4.2
Hep3B	>1000	>1000	38.2	>100	>100
HepG2	>1000	>1000	>100	44.7	>100
Huh7	>1000	218.4	12.1	4.5	20
JHH2	>1000	>1000	>100	61.3	>100
JHH4	>1000	106.9	14.1	1.8	7.2
JHH7	>1000	318	24.7	14.8	28.2
PLC/PRF/5	>1000	277.8	16.7	12.7	22.1
SNU182	>1000	508.1	39.2	22.3	35.9
SNU387	>1000	59.5	4.3	20	40.9
SNU398	>1000	323.5	17.6	2.9	<0.13
SNU423	>1000	226.1	10.8	10.3	18.4
SNU449	>1000	283.4	>100	19.9	>100
SNU475	>1000	584.5	20.5	11.6	29.3

^aHCC cell lines exposed to various agents for 72 h, viability assessed by Cell Titer Glo ($N = 3$). IC₅₀ values determined using Prism4 and expressed in nM.

viability effects correlated with effects on cell cycle distribution, we performed FACS analysis for DNA content on these cells. Consistent with the known cell cycle effects of these compounds, 3 produced a pronounced increase in the percentage of cells in G₂, with a concomitant decrease of cells in the G₁ phase (Figure 9). The effects of aniline 3 were similar to tubulin affecting control compounds (Epothilone, Docetaxel, Vincristine). In contrast, compound 1 at the concentration tested demonstrated no effects on cell cycle distribution, while 2 showed an increase in G₂ and decrease in G₁ populations in

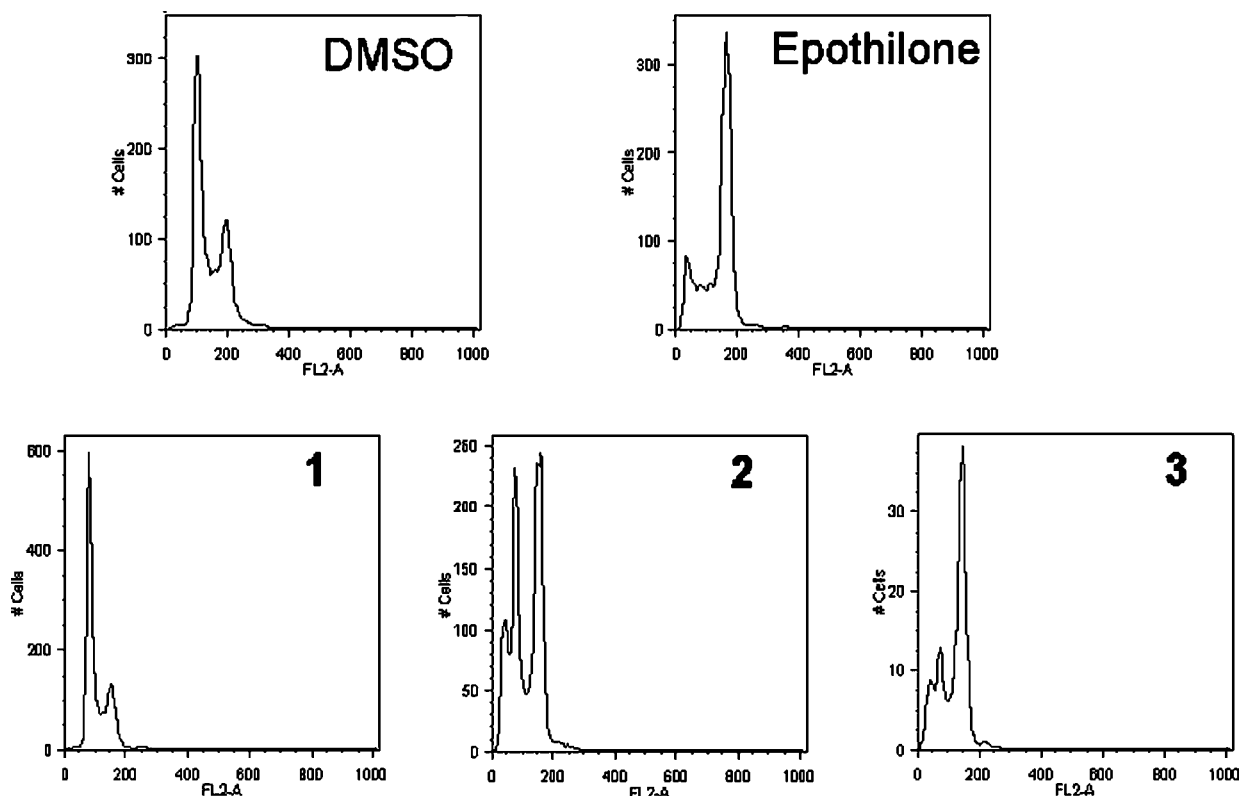


Figure 9. SNU398 FACS Analysis. SNU398 cells were plated and treated with 2 μ M of compounds **1**, **2**, and **3**, or 100 nM (Epothilone) for 24 h before analyzing DNA content via FACS. Epothilone, compounds **3** and **2** show significant G2 arrest, while **1** shows a slight accumulation of G1 cells.

Table 3. FACS Assay Results

compd	SNU398				PLC/PRF/5			
	IC ₅₀ (nM)	%G1	%G2	%sub-G1	IC ₅₀ (nM)	%G1	%G2	%sub-G1
3	94.3	22.9	59.8	13.8	237.4	18.0	67.0	8.4
1	>2000	66.0	30.3	1.0	>2000	65.5	27.1	1.5
2	>2000	33.5	47.8	15.2	>2000	62.8	23.3	8.7
Epothilone	5.0	13.7	70.1	11.8	3.8	5.4	56.3	5.1
Docetaxel	16.6	12.7	72.2	9.3	12.0	11.2	64.4	16.8
Vincristine	46.7	17.1	64.5	14.7	12.7	12.2	68.4	11.8
DMSO	N/A	55.8	38.2	1.2	N/A	66.8	26.1	1.4

SNU398 cells (Table 3). Although this effect of **2** did not manifest in an overt effect on cell viability IC₅₀ in the time frame tested, it may nonetheless indicate a weak tubulin-binding effect.

5. CONCLUSION

In summary, aniline **3** is a substoichiometric tubulin assembly inhibitor which binds to a single site in tubulin with an affinity of $1.1 \times 10^5 \text{ M}^{-1}$ at 25 °C. Compound **3** modifies its fluorescent properties upon tubulin binding which eases binding detection. Excess of podophylotoxin, a colchicine binding site ligand, Vinblastine, Gossipol, Pironetin, or Isohomohalichondrin B, do not displace **3**, indicating a lack of competition for the same binding site. However, excess Nocodazole displaces **3**, indicating the possibility of common binding sites. The amino group at position 7 is essential for this tubulin binding activity because neither aniline **1** nor phenol **2** are able to produce any inhibition of tubulin assembly. Binding inhibition produced by

compound **2** requires at least 1 order of magnitude higher concentration. These binding studies indicate that compound **3** binding site should be close of that of colchicines, possibly between tubulin α/β heterodimer units. STD-NMR studies of tubulin solution with **1** and its 7-aniline derivative **3** also demonstrate that both compounds do not compete for the same site and that the binding conformation of aniline **3** is different from the unbound small-molecule X-ray structure of a related analogue. Finally, antiproliferation of **1** and its derivatives were studied on a panel of hepatocellular carcinoma cell lines, demonstrating that compound **3** is an effective agent against different cell lines and induces a significant G2 arrest during the cell cycle. Unfortunately, aniline **3** showed both microsomal and S9 stability data with less than 5% of the compound remaining, which is in line with the high in vivo clearance observed in rat (above hepatic blood flow of 70 mL/min/kg). Overall, data suggests this compound to be highly cleared in vivo, and efforts are underway to find better long-lived analogues for further efficacy studies.

AUTHOR INFORMATION

Corresponding Author

*E-mail: youssef_Bennani@vrtx.com.

Notes

The authors declare no competing financial interest.

ACKNOWLEDGMENTS

We would like to thank Aixiang Liu and Dewang Wu from Shanghai ChemPartner for resynthesis of compounds **2** and **3**, Juntyma Engrakul, Leena Laitinen, Melina Panitsidis, Dean Wilson, Jingrong Cao, and Kristen Keene for their help. We wish to thank Matadero Municipal Vicente de Lucas de Segovia for providing the calf brains for tubulin purification. This work was supported in part by grants BIO2010-16351, BQU2009-08536 from MICINN (to J.F.D. and J.J.B.) We also acknowledge grants S2011/BMD-2353(MHIT) from Comunidad Autonoma de Madrid (to J.J.B.) and S2010/BMD-2457 (BIPEDD2-CM) from Comunidad Autonoma de Madrid (to J.F.D.).

REFERENCES

- (1) Warolin, C.; Robiquet, P. J. *Rev. Hist. Pharm.* **1999**, *47*, 97–110.
- (2) Dahlstrom, B.; Mellstrand, T.; Lofdahl, C.-G.; Johansson, M. Pharmacokinetic Properties of Noscapine. *Eur. J. Clin. Pharmacol.* **1982**, *22*, 535–539.
- (3) (a) Lettre, H. Synergists and antagonists of mitotic poisons. *Ann. N.Y. Acad. Sci.* **1954**, *58*, 1264–1275. (b) Lettre, H.; Albrecht, M. Narcotin, ein mitosegift (Narcotine, a mitotic poison). *Naturwissenschaften* **1942**, *30*, 184–185.
- (4) (a) Ye, K.; Ke, Y.; Keshava, N.; Shanks, J.; Kapp, J. A.; Tekmal, R. R.; Petros, J.; Joshi, H. C. Opium Alkaloid Noscapine Is an Antitumor Agent That Arrests Metaphase and Induces Apoptosis in Dividing Cells. *Proc. Natl. Acad. Sci. U.S.A.* **1998**, *95*, 1601–1606. (b) Joshi, H. C.; Zhou, J. Noscapine and Analogues as Potential Chemotherapeutic Agents. *Drug News Perspect.* **2000**, *13* (9), 543–546. (c) Ke, Y.; Ye, K.; Grossniklaus, H. E.; Archer, D. R.; Joshi, H. C.; Kapp, J. A. Noscapine Inhibits Tumor Growth with Little Toxicity to Normal Tissues or Inhibition of Immune Responses. *Cancer Immunol. Immunother.* **2000**, *49*, 217–225. (d) Landen, J. W.; Lang, R.; McMahon, S. J.; Rusan, N. M.; Yvon, A.-M.; Adams, A. W.; Sorcinelli, M. D.; Campbell, R.; Bonaccorsi, P.; Ansel, J. C.; Archer, D. R.; Wadsworth, P.; Armstrong, C. A.; Joshi, H. C. Noscapine Alters Microtubule Dynamics in Living Cells and Inhibits the Progression of Melanoma. *Cancer Res.* **2002**, *62*, 4109–4114.
- (5) Aneja, R.; Lopus, M.; Zhou, J.; Vangapandu, S. N.; Ghaleb, A.; Yao, J.; Nettles, J. H.; Zhou, B.; Gupta, M.; Panda, D.; Chandra, R.; Joshi, H. C. Rational design of the microtubule-targeting anti-breast cancer drug EM015. *Cancer Res.* **2006**, *66*, 3782–3791.
- (6) *Cougar Biotechnology Initiates Phase I Trial for CB3304 (Noscapine)*; Cougar Biotechnology, Inc.: Raritan, NJ, December 21, 2007; <http://www.cougarbiotechnology.com/docs/122107Cougar-CB3304PhaseITrialInitiation.pdf> (accessed September 8, 2008).
- (7) Anderson, J. T.; Ting, A. E.; Boozer, S.; Brunden, K. R.; Danzig, J.; Dent, T.; Harrington, J. J.; Murphy, S. M.; Perry, R.; Raber, A.; Rundlett, S. E.; Wang, J.; Wang, N.; Bennani, Y. L. Discovery of S-Phase Arresting Agents Derived from Noscapine. *J. Med. Chem.* **2005**, *48*, 2756–2758.
- (8) Anderson, J. T.; Ting, A. E.; Boozer, S.; Brunden, K. R.; Crumrine, C.; Danzig, J.; Dent, T.; Faga, L.; Harrington, J. J.; Hodnick, W. F.; Murphy, S. M.; Pawlowski, G.; Perry, R.; Raber, A.; Rundlett, S. E.; Stricker-Krongrad, A.; Wang, J.; Bennani, Y. L. Identification of novel and improved antimetabolic agents derived from noscapine. *J. Med. Chem.* **2005**, *48*, 7096–7098.
- (9) Oosawa, F.; Asakura, S. *Thermodynamics of the Polymerization of Protein*; Academic Press: London, 1975; 204pp.
- (10) Ravelli, R. B.; Gigant, B.; Curmi, P. A.; Jourdain, I.; Lachkar, S.; Sobel, A.; Knossow, M. Insight into tubulin regulation from a complex with colchicine and a stathmin-like domain. *Nature* **2004**, *428*, 198–202.
- (11) Xu, K.; Schwarz, P. M.; Luduena, R. F. Interaction of nocodazole with tubulin isotypes. *Drug Dev. Res.* **2002**, *55*, 91–96.